Electro-Optical and Hydrodynamic Properties of Synthetic Polyribonucleotides in Solutions as Studied by Electric Birefringence

Masato Tanigawa and Kiwamu Yamaoka*

Department of Material Science, Faculty of Science, Hiroshima University,
1-3-1 Kagamiyama, Higashi-Hiroshima 724

(Received July 8, 1994)

The electro-optical and hydrodynamic properties of four synthetic polyribonucleic acids were clarified by electric birefringence methods which take the molecular-weight distribution into consideration. Parallel double-stranded helices, poly(adenylic acid)·poly(protonated adenylic acid), **I**, and poly(cytidylic acid)·poly(protonated cytidylic acid), **II**, are known to possess an electric permanent dipole moment, because the reversing-pulse electric birefringence (RPEB) signals of these duplexes exhibit dips upon pulse reversal. The RPEB signals of antiparallel double-stranded poly(adenylic acid)·poly(uridylic acid), **III**, and poly(guanylic acid)·poly(cytidylic acid), **IV**, show no dip; therefore, these polynucleotides have no permanent dipole moment. By analyzing the relaxation time of the birefringence decay signals, the axial translations of the polynucleotides per base-pair were determined to be 4.0 Å for **I**, 2.7 Å for **III**, and 2.4 Å for **IV**, respectively. By analyzing the dependence of the steady-state birefringence values on the electric-field strength, the magnitudes of the permanent dipole moments per unit length of **I** and **II** projected onto the helix axes were found to be ca. 0.4 debye $Å^{-1}$. The electric properties unraveled by electric birefringence experiments were compared with calculations based on a recent Manning theory. An unsaturable induced dipole moment may result from the polarization of the Debye–Hückel ion-atmosphere, while a saturable induced dipole moment is probably caused by the polarization of counter ions that are condensed on the charged sites of a polyion. The experimental values deviate from calculated values at ionic strengths lower than 0.0001; hence, the Manning theory is not applicable in this region.

In aqueous solutions, DNA and RNA are ionized with high electrical density. It would be interesting to clarify the electrostatic interaction of these polyions with counter ions and co-ions in solution. Mandel[1] clarified the electric polarizability of polyions at low filed strength, neglecting the mutual repulsion between counter ions. Based on the idea that electric polarizability arises from ion fluctuation, Oosawa[2,3] has discussed in detail the polarizability of a polyelectrolyte in solution. Archer et al.[4] have studied the extent of binding of counter ions to synthetic polynucleotides. Rau and Charney[5] studied the polarizability of an ion-atmosphere based on the Debye–Hückel theory. Many investigations have been carried out concerning the behavior of counter ions and co-ions around polyions, and also for the electric properties of a polymer solution by computer simulations.[6—9] Manning[10,11] has suggested that counter ions are condensed on polyions, and that the electric polarizability is caused by both counter-ion condensation on polyions and by a Debye–Hückel-type interaction of counter ions with polyions[12—14] when the charge density of the polyion is high.

Electric birefringence is a very useful technique for studying the magnitude and nature of the electric moments of polymers in solution.[15—25] If polymers with electrical and optical axes of symmetry have no permanent electric dipole moment (μ), the field-strength dependence of steady-state birefringence ($\Delta n(E)$) of the polymer can be analyzed, by using a saturable and unsaturable induced dipole (SUSID) orientation function.[23,24] This function presupposes that a rodlike polymer is oriented due to an interaction between an applied external field (E) and both an unsaturable induced electric dipole moment ($\Delta\alpha' E$), which is proportional to the field strength, and a saturable induced electric dipole moment ($\Delta\sigma E_0$), which is saturated at a critical field strength (E_0) and becomes constant above this point.[26—29] If a polyion has a permanent dipole moment, the electric properties of the molecule can be analyzed, by using the permanent dipole, the saturable and unsaturable induced dipole (PD-SUSID) orientation function, i.e., an extended function for a molecule having three electric moments ($\Delta\alpha' E$, $\Delta\sigma E_0$ and μ).[25] Since a polymer sample generally has a molecular-weight distribution, it is necessary to consider such a distribution for analyzing the electrical properties of the system. It is thus desirable to determine the molecular-weight distribution independently of electric bire-

fringence experiments. The present authors extended the PD-SUSID orientation function for the polydisperse system and clarified the importance of the molecular-weight distribution for studying the electrical properties, proposing a practical method of analysis.[30]

In this work four synthetic polynucleotides were studied: poly(adenylic acid)·poly(protonated adenylic acid) (abbreviated as $(A)_n\cdot(A^+)_n$) and poly(cytidylic acid)·poly(protonated cytidylic acid) (abbreviated as $(C)_n\cdot(C^+)_n$), which are in a singly charged double-helical structure in acid solutions,[31—40] as well as poly(adenylic acid)·poly(uridylic acid) (abbreviated as $(A)_n\cdot(U)_n$) and poly(guanylic acid)·poly(cytidylic acid) (abbreviated as $(G)_n\cdot(C)_n$), which are formed in neutral-pH solutions.[41—45] Since each sample is constituted from base pairs of the single type and the molecular structure is uniformly defined, the electric properties are reflected by the structure with a specific base-pair. Both $(A)_n\cdot(U)_n$ and $(G)_n\cdot(C)_n$ are antiparallel-stranded helices like DNA, and the permanent electric dipole moments are compensated. On the other hand, $(A)_n\cdot(A^+)_n$ and $(C)_n\cdot(C^+)_n$ are parallel-stranded helices and may have a permanent dipole moment in the direction of the symmetry helix axis.

The purpose of this study was to clarify the electro-optical properties of the above-cited four polyribonucleotides by using the PD-SUSID orientation function for the polydisperse system. For this purpose, these molecular parameters were determined independently by the gel-permeation-chromatography/low-angle-laser-light-scattering (abbreviated as GPC/LALLS) method. The weight-average rotational relaxation time was evaluated based on the transient birefringence decay signals to obtain the hydrodynamic properties using the procedure for extrapolating the relaxation times at given fields to infinitely high fields while considering the electric property and molecular-weight distribution. The chain lengths of each double stranded helix were estimated based on the weight-average rotational relaxation times. The counter ions were sodium and magnesium ions at varying ionic strengths from 1.0×10^{-4} to 1.0×10^{-3}; the relationship between the electrical properties and the chain lengths was examined. These results were compared with the Manning theory, the validity of which is also discussed.

Experimental

Materials. Polyribonucleotide samples were prepared in the same way as previously described by Tanigawa et al.[46] The following samples were purchased from, or kindly supplied by, Yamasa Shoyu Co., Ltd. (Choshi, Chiba, Japan). Duplex $(A)_n\cdot(A^+)_n$ was prepared by dissolving $(A)_n$ (lot no. S-101) in an acetic acid buffer maintained at a pH of 5.5 and an ionic strength of 0.0871; $(C)_n\cdot(C^+)_n$ was prepared by dissolving $(C)_n$ (lot no. 301430) in a 0.1 mol dm^{-3} NaCl solution maintained at a pH of 4.6 with an acetic acid buffer and at an ionic strength of 0.15; $(A)_n\cdot(U)_n$ (lot no. 2-7) was dissolved in a 0.1 mol dm^{-3} NaCl solution at a neutral pH. $(G)_n\cdot(C)_n$ was prepared by mixing $(G)_n$, purchased from Sigma Chemical Co. (U. S. A.) (lot no. 18F-4026), with $(C)_n$, supplied from Yamasa Shoyu Co., Ltd. (lot no. S-301) in a 0.1 mol dm^{-3} NaCl solution maintained at a pH of 8 with sodium phosphate buffer and at an ionic strength of 0.15. All other chemicals were of reagent grade.

In order to prepare rodlike narrowly-polydisperse samples, ultrasonic irradiation was carried out in the same way as described by Fukudome et al.[47,48] with a Tomy Model UR-200P sonicator (Tomy Seiko Co. (Tokyo)) at an output power level of 200 watts (20 kHz) for a total of 20 min (forty repetitions of a 30-s burst and subsequent 5-min bubbling interval) under a helium gas atmosphere. Although the concentration of the polymer solution was usually 2.0 mg cm^{-3}, 1.5 mg cm^{-3} was used for $(A)_n\cdot(A^+)_n$. The intactness of each sample was confirmed by the UV-absorption spectra, which showed no change before or after sonication.[49,50] All sonicated sample solutions were fractionated to several fractions at 20 °C by the successive precipitational method with acetone being used as the precipitant in the same way as described by Fukudome et al.[47,48]

Prior to GPC/LALLS and electric birefringence measurements, each fraction was dialyzed at 4 °C over a period of 48 h against an appropriate solvent at a total of 4 dm^3 (several batches were changed), the first batch containing 0.1 mol dm^{-3} ethylenediaminetetraacetate (disodium salt). Although a singly charged $(A)_n\cdot(A^+)_n$ helix is said to form in an acetic acid buffer maintained at a pH of 5.5 and an ionic strength of 0.1, a doubly charged $(A^+)_n\cdot(A^+)_n$ is probably formed in the same buffer maintained at a pH of 4.0 and an ionic strength of 0.1.[33,40,51,52] Figure 1 shows the CD-spectra of duplexes comprising $(A)_n$ in acetic acid buffers maintained at pHs of 5.5 and 4.0 and at ionic strengths of 0.1 and 0.001. The measurements were performed on a JASCO J-600 spectropolarimeter at room temperature. It was clear that singly charged $(A)_n\cdot(A^+)_n$ duplexes, formed at two ionic strengths of 0.001 and 0.1, were in the same conformation if the pH was maintained at 5.5.

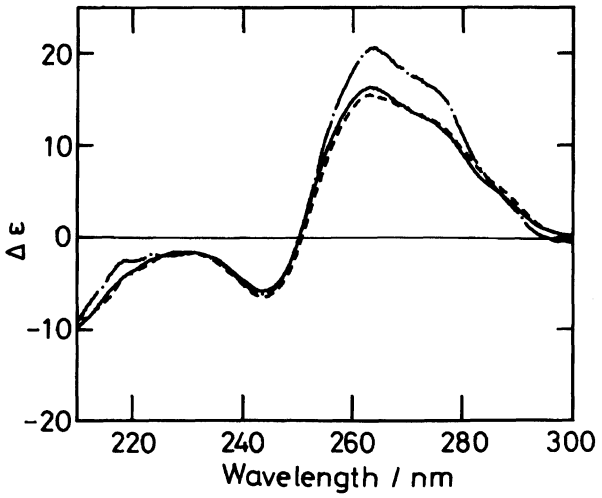

Fig. 1. Circular dichroism of duplexes composed of $(A)_n$. The molar dichroism $\Delta\epsilon$ is expressed with mol^{-1} dm^3 cm^{-1}. (—): I_s=0.001, pH 5.5. (---): I_s=0.1, pH 5.5. (-·-): I_s=0.001, pH 4.0. I_s is the ionic strength.

Measurements of GPC/LALLS. Measurements of the molecular weight and molecular-weight distribution profiles of the samples were carried out, as described in detail in a previous study,[46] at 30 °C on a Tosoh flow-type GPC/LALLS detecting system (Tosoh Co. (Tokyo)), which consists of two Tosoh TSK G-DNA-PW columns in tandem, a Tosoh LS-8000 light-scattering photometer, and a Tosoh RI-8011 differential refractometer. A sample solution (0.5 cm^3) at a concentration of 0.114—2.33 mg cm^{-3} was injected for a single run at a flow rate of 0.6 cm^3 min^{-1}. The eluting solution was filtered through a sintered stainless filter for the GPC columns, and through a 0.45 μm pore-size cellulose acetate membrane (Millipore Co., HAWP 01300) in front of the LALLS apparatus for complete removal of any dust. A bovine serum albumin sample from Miles Inc., Diagnostics Div., (U.S.A.), and a chicken erythrocyte nucleosomal DNA fragment (molecular weight=95700) were used as the molecular-weight standard. Because of an aggregating tendency, the strands of $(C)_n{\cdot}(C^+)_n$ were separated at a pH of 8 and an ionic strength of 0.1 in a phosphate buffer. The molecular weight was determined as a single strand and then multiplied by a factor of 2. $(A)_n{\cdot}(A^+)_n$ duplexes were measured in a 0.05 mol dm^{-3} NaCl solution at a pH of 5.5, then adjusted with an acetate buffer and at an ionic strength of 0.1. The remaining samples were all measured as double-strands under the same conditions as described in **Materials**.

Measurements of Electric Birefringence. Electric birefringence was measured at 7 °C and at 633 nm on a He–Ne laser apparatus with a quarter-wave plate in the optical path; the details were given in a previous paper.[53] The residue concentrations of samples, expressed in terms of mononucleotide units, were diluted in the (0.08—0.17) mmol dm^{-3} range. The counter ion was either Na^+ or Mg^{2+}, and the ionic strength was kept in the $(0.1—1.0)\times10^{-3}$ range by dialysis. In order to improve the signal-to-noise ratio, the birefringence signal was digitized on a 10-bit wave memory (Riken Denshi TCL-005-4000R), accumulated, and processed on a microcomputer (NEC PC9801VM). The Kerr cells were of the cylindrical type, their optical paths (d) being 1.00 cm (electrode gap of 2.0 mm) and 3.00 cm (electrode gap of 4.2 mm).

The electric birefringence (Δn) is expressed with the optical phase retardation (δ), which is experimentally determined as

$$\Delta n = n_{//} - n_{\perp} = \frac{\lambda}{2\pi d}\delta = 2\pi C_v \left(\frac{\Delta g}{n}\right) \Phi(E), \qquad (1)$$

where λ is the wavelength in vacuo, C_v the volume fraction of the solute, $\Delta g/n$ the reduced optical anisotropy factor, n the refractive index of the solution, and $\Phi(E)$ the orientation function.[17]

Analysis of Electric Birefringence

Steady-State Data. The steady-state values of the electric birefringence for polydisperse systems were analyzed by using the theoretical PD-SUSID orientation function, while taking the molecular-weight distribution into consideration.[30] The total electric dipole moment (m_t) of an ionized polymer is given by[25]

$$m_t = \mu + \Delta\alpha' E + \Delta\sigma E \qquad (0 < E \leq E_0), \qquad (2)$$

$$m_t = \mu + \Delta\alpha' E + \Delta\sigma E_0 \qquad (E_0 \leq E), \qquad (3)$$

where $\Delta\alpha'(=\alpha'_{33}-\alpha'_{11})$ is the electric polarizability anisotropy responsible for the unsaturable electric dipole moment ($\Delta\alpha' E$), α'_{33} and α'_{11} being the polarizabilities along the longitudinal and transverse axes. $\Delta\sigma(=\sigma_{33}-\sigma_{11})$ is the electric polarizability anisotropy responsible for the saturable dipole moment ($\Delta\sigma E_0$), which is saturated at the critical electric filed strength (E_0), the symmetry axis being taken as the 3 axis. Polyion molecules in solution are oriented as a result of an interaction between the external electric field and the electric moments of the molecules. The potential energy (W) is expressed as

$$W = -\mu E - \frac{1}{2}(\Delta\alpha' + \Delta\sigma)E^2 \qquad (0 < E \leq E_0), \qquad (4)$$

$$W = -\mu E - \Delta\sigma E_0 E - \frac{1}{2}\Delta\alpha' E^2 + \frac{1}{2}\Delta\sigma E_0^2 \qquad (E_0 \leq E). \qquad (5)$$

By using these terms, the PD-SUSID orientation function ($\Phi(\beta, \rho_s, \rho, \gamma')$) was calculated with the following parameters:[25]

$$\beta = \frac{\mu E}{kT}, \rho_s = \frac{\Delta\sigma E_0 E}{kT}, \rho = \frac{\Delta\sigma E^2}{2kT}, \gamma' = \frac{\Delta\alpha' E^2}{2kT}. \qquad (6)$$

This PD-SUSID orientation function was extended to the polydisperse system.[30] The weight-average orientation function ($\langle\Phi(\beta, \rho_s, \rho, \gamma')\rangle_w$) is defined as

$$\langle\Phi(\beta,\rho_s,\rho,\gamma')\rangle_w = \frac{\int\Phi(M)f_w(M)dM}{\int f_w(M)dM}, \qquad (7)$$

where $f_w(M)$ is the weight fraction of molecules with molecular weight (M). In the present work, the weight-average PD-SUSID orientation function was calculated with the logarithmic-normal distribution function for $f_w(M)$.[46] The weight-average electric property of a given polydisperse system was evaluated by fitting the theoretical PD-SUSID orientation function to the electric birefringence steady-state values, measured over a wide range of field strengths.[25]

Decay Process. The birefringence decay process commences upon removal of an applied pulse field of arbitrary strength. The area surrounded by the normalized decay curve and baseline yields the electric birefringence-average relaxation time ($\langle\tau\rangle_{EB}$; the area method):[54—56,59]

$$\langle\tau\rangle_{EB} = \int_0^\infty \frac{\Delta n(t)}{\Delta n(0)}dt = \frac{\int\tau(M)\Phi(M)f_w(M)dM}{\int\Phi(M)f_w(M)dM}, \qquad (8)$$

where $\tau(M)$ is the rotational relaxation time of a molecule with a molecular weight of M. For a rodlike molecule, τ is expressed by Broersma[55] as

$$\tau = \frac{\pi\eta_0 L^3}{18kT}\left[\ln\left(\frac{L}{b}\right) - 1.57 + 7\left(\frac{1}{\ln\left(\frac{L}{b}\right)} - 0.28\right)^2\right]^{-1}, \qquad (9)$$

where η_0 is the viscosity of the solvent, L the length of cylindrical molecules, and b the radius of the cylinder. Since $\Phi(M)$ approaches unity at infinitely high

fields, $\langle\tau\rangle_{EB}$ reduces to the weight-average relaxation time ($\langle\tau\rangle_w$).[56,57]

Results

Reversing-Pulse Electric Birefringence. Figure 2 shows some reversing-pulse electric birefringence signals of $(A)_n\cdot(A^+)_n$, $(C)_n\cdot(C^+)_n$, $(A)_n\cdot(U)_n$, and $(G)_n\cdot(C)_n$ in the low electric field region. Each signal of $(A)_n\cdot(A^+)_n$ and $(C)_n\cdot(C^+)_n$ shows a dip upon field reversal (arrow in a and b). Such a signal may appear, if a rodlike polymer possesses a permanent dipole or an ion-induced dipole moment whose induction time is comparable to the rotational relaxation time of the whole molecule.[22,24,58] Therefore, parallel double-stranded $(A)_n\cdot(A^+)_n$ and $(C)_n\cdot(C^+)_n$ probably possess a permanent dipole and/or slow-induced dipole moments. Since the signals of antiparallel double stranded $(A)_n\cdot(U)_n$ and $(G)_n\cdot(C)_n$ show no dip upon field reversal (arrow in c and d), these duplexes possess neither a permanent dipole nor a slow-induced dipole moment.

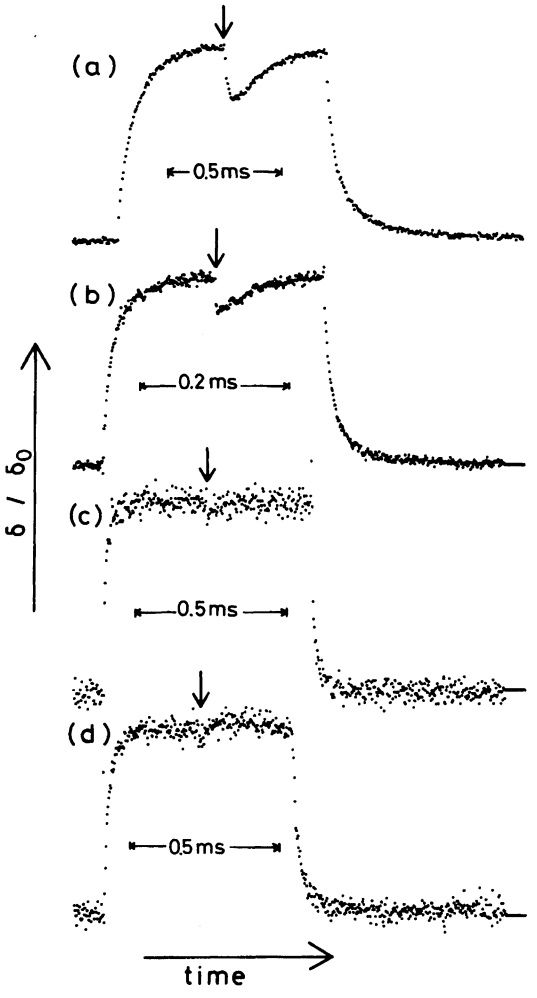

Fig. 2. Normalized RPEB singles (δ/δ_0) of four duplexes with Na^+ counter ions at 7 °C and at 633 nm. (a) $(A)_n\cdot(A^+)_n$ (I_s=0.001, M_w=1.88×10^5, δ_0=−1.0 deg, E=0.9 kV cm^{-1}). (b) $(C)_n\cdot(C^+)_n$ (I_s=0.0008, M_w=2.45×10^5, δ_0=−0.65 deg, E=2.1 kV cm^{-1}). (c) $(A)_n\cdot(U)_n$ (I_s=0.001, M_w=1.21×10^5, δ_0=−0.17 deg, E=1.0 kV cm^{-1}). (d) $(G)_n\cdot(C)_n$ (I_s=0.001, M_w=1.85×10^5, δ_0=−0.18 deg, E=0.7 kV cm^{-1}). M_w is the weight average molecular weight.

Field-Strength Dependence of Steady-State Birefringence. Figure 3 shows the dependence of the steady-state optical phase retardation (δ) of $(A)_n\cdot(A^+)_n$ on the electric field strength. The intrinsic optical phase retardation values ($\delta(\infty)$) given in Table 1 were obtained by extrapolating the δ values to infinitely high fields with the aid of the theoretical PDSUSID orientation function for the polydisperse system (the fitting method).[23] Since the intrinsic optical phase retardation values of $(A)_n\cdot(A^+)_n$ are 152±9 deg mmol^{-1} dm^3 cm^{-1} and the variation with the ionic strength is small, it is safe to conclude that the secondary structure does not change with the conditions cited. Regardless of counter ions, the degree of orientation becomes lower; hence, the induced dipole moment becomes smaller as the ionic strength increases. At a given ionic strength, the degree of orientation in the middle-to-high field region is smaller for the counter ion Na^+ than for Mg^{2+}.

The possible transformation of the field-strength dependence of the electric birefringence from the second- to first-power (E^2 to E^1) can be visualized more effectively if the optical phase retardation, which is normal-

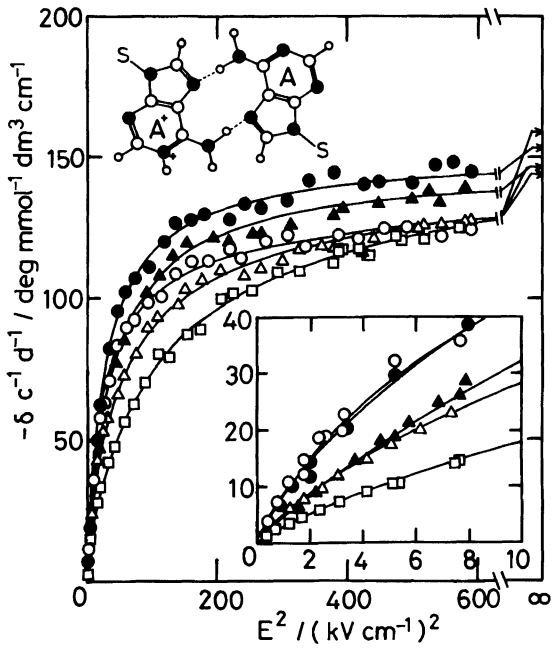

Fig. 3. Dependence of the steady-state optical phase retardation per residue concentration and pathlength, δ/cd, in deg mmol^{-1} dm cm^{-1} on the applied electric field strength for $(A)_n\cdot(A^+)_n$ with Na^+ or Mg^{2+} counter ions. M_w is 1.88×10^5. (○) (Na^+, I_s=0.0001); (●) (Mg^{2+}, I_s=0.0001); (△) (Na^+, I_s=0.0004); (▲) (Mg^{2+}, I_s=0.0004); (□) (Na^+, I_s=0.001).

Table 1. Experimental and Calculated Electric Properties of Four Double-Stranded Polyribonucleotides

Duplexes	Counter-ions	Ionic strengths	$\delta_\infty \cdot c^{-1} \cdot d^{-1}$ deg mM^{-1} cm^{-1}	μ 10^{26} C cm^{-1}	$\Delta\alpha$ 10^{33}F m Obsd	$\Delta\alpha$ 10^{33}F m Calcd[a]	$\Delta\sigma$ 10^{33}F m	E_0 kV cm^{-1}	$\Delta\sigma E_0$ 10^{26}C m Obsd	$\Delta\sigma E_0$ 10^{26}C m Calcd[a]
Poly(A)·Poly(A$^+$)										
M_w=3.39×10^5	Na$^+$	0.0001	−152.0	2.10	9.67	646	1230	0.27	2.07	0.32
(1.53)[b]		0.0010	−161.0	1.20	6.29	77.7	399	0.47	1.18	1.26
	Mg^{2+}	0.0001	−158.0	2.42	155	—[c]	1620	0.23	2.38	0.76
M_w=1.88×10^5	Na$^+$	0.0001	−144.0	1.43	4.85	469	357	0.98	2.24	0.46
(1.52)		0.0004	−147.0	1.20	12.6	117	198	0.93	1.18	0.50
		0.0010	−159.0	1.03	8.64	42.8	97.2	0.94	0.58	0.43
	Mg^{2+}	0.0001	−153.0	1.37	49.7	—	518	0.41	1.35	0.20
		0.0004	−147.0	1.49	55.4	—	61.7	1.18	0.46	0.66
M_w=5.97×10^4	Na$^+$	0.0001	−142.8	0.51	0.61	188	45.2	2.77	0.80	0.09
(1.34)		0.0010	−158.6	0.57	2.70	15.2	15.2	3.37	0.33	0.12
	Mg^{2+}	0.0001	−155.0	0.42	4.97	—	25.9	2.58	0.43	0.06
Poly(C)·Poly(C$^+$)										
M_w=4.47×10^5	Na$^+$	0.0010	−60.2	1.00	0.75	26.9	4.64	6.10	0.18	0.53
(1.56)	Mg^{2+}	0.0010	−61.5	0.84	0.56	—	3.94	14.8	0.37	1.93
M_w=2.45×10^5	Na$^+$	0.0008	−50.0	0.69	3.97	34.4	31.4	2.85	0.67	0.29
(1.33)	Mg^{2+}	0.0008	−57.0	0.60	3.03	—	9.59	8.17	0.59	0.90
M_w=1.69×10^5	Na$^+$	0.0010	−50.6	0.55	2.46	21.4	6.83	6.12	0.31	0.30
(1.39)	Mg^{2+}	0.0010	−49.0	0.43	4.66	—	4.89	11.4	0.42	0.68
Poly(A)·Poly(U)										
M_w=3.85×10^5	Mg^{2+}	0.0010	−112.0	0	9.48	—	53.0	3.47	1.38	2.49
(1.35)										
M_w=1.21×10^5	Mg^{2+}	0.0004	−95.0	0	4.98	—	26.4	8.09	1.36	0.59
(1.46)		0.0010	−95.7	0	6.79	—	10.6	6.99	0.47	0.31
Poly(G)·Poly(C)										
M_w=1.85×10^5	Na$^+$	0.0008	−110.0	0	16.4	36.1	50.2	3.21	1.03	0.40
(1.58)	Mg^{2+}	0.0008	−118.6	0	2.20	—	23.3	6.09	0.90	0.37

a) These values are calculated with Eqs. 12 and 13. b) Values in parenthese are the polydispersity M_w/M_n. c) Eq. 12 is not applicable for divalent salt.

ized by the concentration of the sample and the optical path length, is plotted against the applied electric field strength on a double-logarithmic scale.[56] Figure 4 shows such plots. The slopes of the straight lines of low-weight samples (circles and triangles) are found to be two. Thus, Kerr's law (E^2-dependence) holds in the low-to-middle field region. The slopes of the straight lines of the high-weight samples are found to be unity in the low-field region. As the SUSID orientation function indicates,[30,60] the electric birefringence is linear with respect to the first, but not to the second power of the electric field strength (E), if the applied field is higher than the critical field strength (E_0). This E^1-dependence of δ was already observed for high-weight DNA samples.[60] The degree of orientation of $(A)_n \cdot (A^+)_n$ with the counter ion Na^+ is larger than that with Mg^{2+} at very weak fields, though the trend is reversed in the middle-to-high field region.

Figure 5a shows the dependence of the steady-state optical phase retardation of $(C)_n \cdot (C^+)_n$ on the electric field strength (E). The intrinsic optical phase retardation values ($\delta(\infty)$), which are obtained by the curve-fitting method with the PD-SUSID orientation function, are 55±6 deg mmol^{-1} dm^3 cm^{-1}. As for $(A)_n \cdot (A^+)_n$, although the degree of orientation of $(C)_n \cdot (C^+)_n$ is larger with the Na^+ counter ion than with the Mg^{2+} ion at the low-field region, the trend is reversed in the middle-to-high field region. Figure 5b shows the dependence of the steady-state optical phase retardation of $(A)_n \cdot (U)_n$ on the electric field strength. Like $(A)_n \cdot (A^+)_n$, the degree of orientation is larger with decreasing ionic strengths; hence, the lower is the ionic strength, the larger is the ion-induced dipole moment. Figure 5c shows the dependence of the steady-state optical phase retardation of $(G)_n \cdot (C)_n$ on the electric field strength. As in the cases of other polyribonucleotides, the degree of orientation of $(G)_n \cdot (C)_n$ is larger with the Mg^{2+} counter ion than with Na^+ in the middle-to-high field region.

Rotational Relaxation Time. Figure 6 shows the dependence of the electric birefringence-average rotational relaxation time ($\langle\tau\rangle_{EB}$) on the electric field strength for $(A)_n \cdot (A^+)_n$ and $(A)_n \cdot (U)_n$. The solid lines were calculated with Eq. 8 based on the assumption that τ is proportional to the cube of L. These curves represent the measured values quite well. This result indicates that these duplexes are oriented according to the PD-SUSID orientation mechanism. The weight-av-

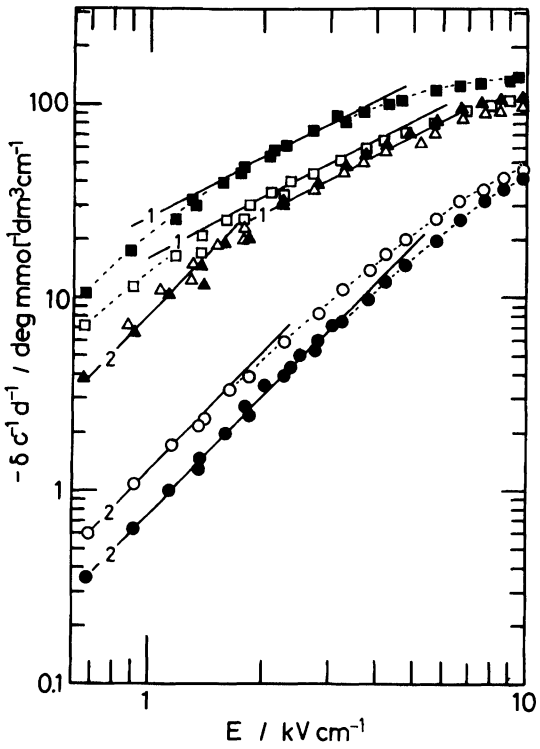

Fig. 4. Double-logarithmic plots of the steady-state optical phase retardation values for $(A)_n\cdot(A^+)_n$ with Na^+ or Mg^{2+} counter ions versus the applied electric field strength. The ionic strength is 1.0×10^{-4}. (○) (Na^+, $M_w=5.97\times10^4$); (●) (Mg^{2+}, $M_w=5.97\times10^4$); (△) (Na^+, $M_w=1.88\times10^5$); (▲) (Mg^{2+}, $M_w=1.88\times10^5$); (□) (Na^+, $M_w=3.39\times10^5$).

erage rotational relaxation time ($\langle\tau\rangle_w$) is estimated, by extrapolating values of $\langle\tau\rangle_{EB}$ to infinitely high fields by using this curve. Taking the molecular weight distribution of a polydisperse sample into account, the weight-average chain length ($\langle L\rangle_w$) was determined from $\langle\tau\rangle_w$ with Eq. 9, in which the molecules were assumed to be rodlike. In the extremely high-field region, the PD-SUSID orientation function can be expanded as:[25]

$$\Phi(\beta^2\gg1,\rho_s^2\gg1,\gamma'\gg1)=1-\frac{3}{(\beta+\rho_s)+2\gamma'} \qquad (E>E_0), \quad (10)$$

$$\Phi(\beta^2>>1,(\rho+\gamma')>>1)=1-\frac{3}{\beta+2(\rho+\gamma')} \qquad (E<E_0), \quad (11)$$

Equations 9, 10, and 11 indicate that $\langle\tau\rangle_{EB}$ approach $\langle\tau\rangle_w$ linearly against the reciprocal of the field strength (E^{-1}) if the permanent and saturable-induced dipole moments contribute mostly to the field orientation. Since the weight-average molecular weight of the smallest $(A)_n\cdot(A^+)_n$ sample is 5.97×10^4 (too small to be separated by the GPC column), this extrapolation method is applied to estimating $\langle\tau\rangle_w$ for this sample, by plotting $\langle\tau\rangle_{EB}$ against E^{-1}.

The axial translation of a duplex chain per base-pair (h) can be calculated, by dividing $\langle L\rangle_w$ by the number of weight-average base-pairs ($\langle bp\rangle_w$), which is in turn calculated, by dividing the weight-average molecular weight ($\langle M\rangle_w$) by the molecular weight of a nucleotide, which is 694 for $(G)_n\cdot(C)_n$, 679 for $(A)_n\cdot(U)_n$, 654 for $(C)_n\cdot(C^+)_n$, and 702 for $(A)_n\cdot(A^+)_n$. Table 2 gives the values of $\langle\tau\rangle_w$, $\langle L\rangle_w$ and h for all of the duplexes. The axial translations per base-pair are (6.8—10) Å for $(A)_n\cdot(A^+)_n$ at 0.001 of the ionic strength of Mg^{2+}. These extraordinarily large values indicate that $(A)_n\cdot(A^+)_n$ aggregates in this condition.

Figure 7 shows the axial translation per base-pair (h) plotted against the weight-average molecular weight ($\langle M\rangle_w$) for each polynucleotide duplex. The value becomes smaller with increasing $\langle M\rangle_w$, probably because of the bending effect of the helical chain, which should be more notable for higher molecular-weight duplexes. The solid lines were fitted to the observed axial translations per base-pair for $(A)_n\cdot(A^+)_n$ and $(C)_n\cdot(C^+)_n$ by the least-squares method. The dashed lines were drawn parallel to the solid lines which pass through the points for $(A)_n\cdot(U)_n$ and $(G)_n\cdot(C)_n$. The value of h, extrapolated to the limiting low molecular weight, is 4.0 Å for $(A)_n\cdot(A^+)_n$. This value is very close to 3.8, which was estimated from on X-ray study.[34] Similarly, the h values extrapolated to the ordinate ($M_w\to0$) are 2.7 Å for $(A)_n\cdot(U)_n$, 2.4 Å for $(G)_n\cdot(C)_n$, and 2.1 Å for $(C)_n\cdot(C^+)_n$. The value of $(A)_n\cdot(U)_n$ is in good agreement to 2.8 Å;[44] however, the value for $(C)_n\cdot(C^+)_n$ is smaller than 3.1 Å, estimated from an X-ray study.[36] Since the degree of flexibility of $(C)_n\cdot(C^+)_n$ may be large, as clarified from a viscosity study,[46] the extrapolated value must be smaller than the value for rodlike $(C)_n\cdot(C^+)_n$.

Discussion

Persistent Length of the Duplex. Hagerman and Zimm[61] derived the following equation for the persistent length (P) and the experimental relaxation time (τ_a):

$$\frac{\tau_a}{\tau_b}=(1.0120-0.24813X+0.03703X^2-0.019177X^3)\times(1-Y)$$
$$Y=0.06469X-0.01153X^2+0.0009893X^3, \qquad (12)$$

where τ_b is the rotational relaxation time of a straight cylinder, and X ($=L/P$) is the ratio of the contour length (L) to persistent length (P). Figure 8 shows the variation of ratio τ_a/τ_b with L for $(A)_n\cdot(A^+)_n$ and $(C)_n\cdot(C^+)_n$. This ratio can be fitted to the calculated lines with a persistent length of 550 Å for $(A)_n\cdot(A^+)_n$ and that of 250 Å for $(C)_n\cdot(C^+)_n$. This result means that the persistent length of a parallel-stranded duplex of polyribonucleotides depends on the type of base pairs.

Electrical Property. The electrical parameters ($\langle\mu\rangle_w$, $\langle\Delta\alpha'\rangle_w$, $\langle\Delta\sigma\rangle_w$, $\langle E_0\rangle_w$, and $\langle\Delta\sigma\rangle_w\cdot\langle E_0\rangle_w$) are given in Table 1. These values were estimated, by fitting the theoretical PD-SUSID function for the polydisperse system to the steady-state electric birefringence,

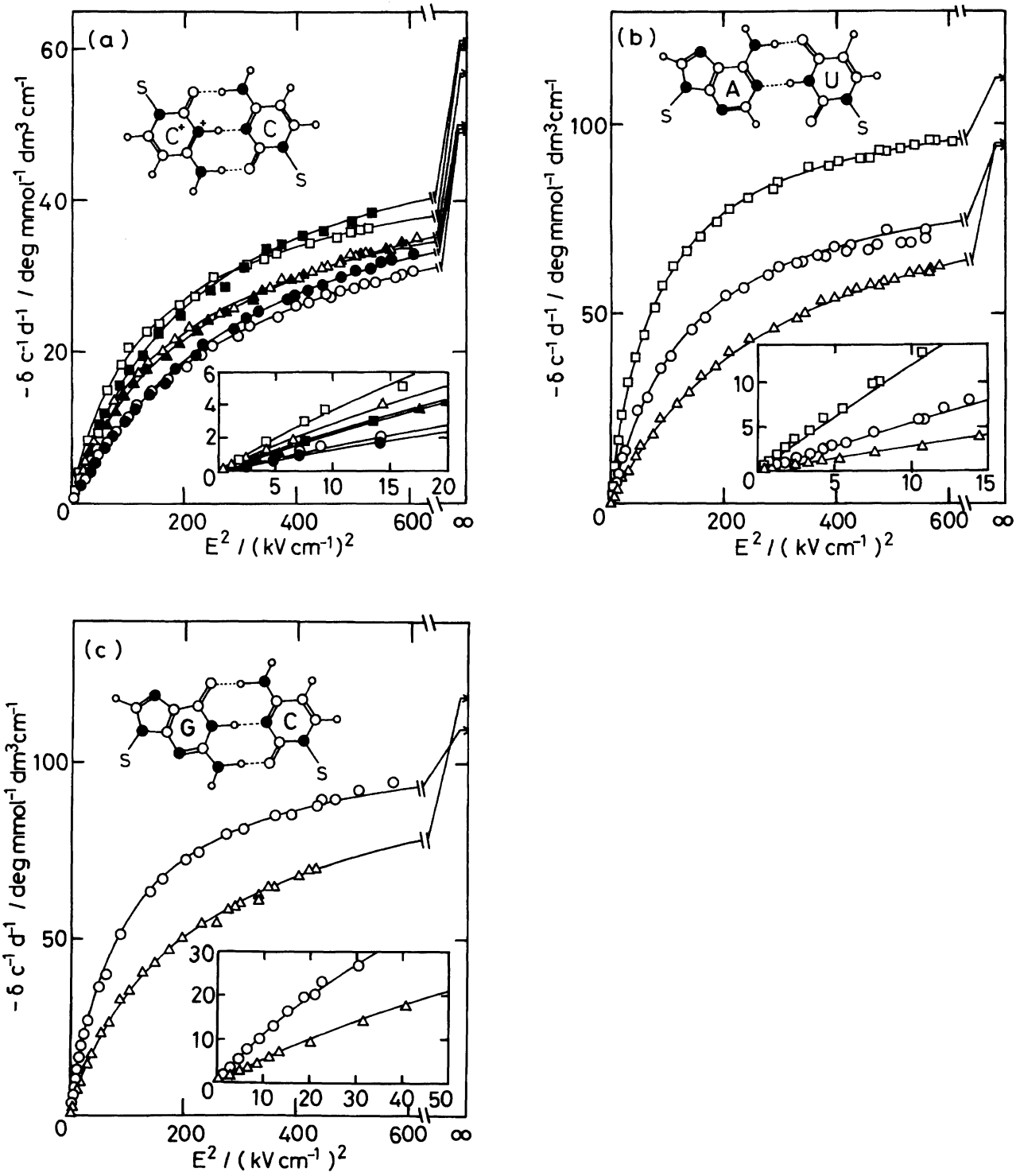

Fig. 5. Dependence of the steady-state optical phase retardation on the applied electric field strength for $(C)_n\cdot(C^+)_n$, $(G)_n\cdot(C)_n$ and $(A)_n\cdot(U)_n$ with Na^+ or Mg^{2+} counter ions. (a) $(C)_n\cdot(C^+)_n$: (○) (M_w=1.69×10^5, Na^+, I_s=0.001); (△) (M_w=4.47×10^5, Na^+, I_s=0.001); (□) (M_w=2.45×10^5, Na^+, I_s=0.0008); (●) (M_w=1.69×10^5, Mg^{2+}, I_s=0.001); (▲) (M_w=4.47×10^5, Mg^{2+}, I_s=0.001); (■) (M_w=2.45×10^5, Mg^{2+}, I_s=0.0008). (b) $(A)_n\cdot(U)_n$, (○) (M_w=1.21×10^5, Mg^{2+}, I_s=0.001); (△) (M_w=3.85×10^5, Mg^{2+}, I_s=0.001); (□) (M_w=1.21×10^5, Mg^{2+}, I_s=0.0004). (c) $(G)_n\cdot(C)_n$: (○) (M_w=1.85×10^5, Na^+, I_s=0.0008); (△) (M_w=1.85×10^5, Mg^{2+}, I_s=0.0008).

shown in Figs. 3 and 5. Clearly, the parallel helices, $(A)_n\cdot(A^+)_n$ and $(C)_n\cdot(C^+)_n$, have permanent dipole moments of reasonable magnitudes, as is also supported by reversing-pulse birefringence signals. Antiparallel helices, $(A)_n\cdot(U)_n$ and $(G)_n\cdot(C)_n$, have no permanent dipole moment, as expected from the fact that the re-

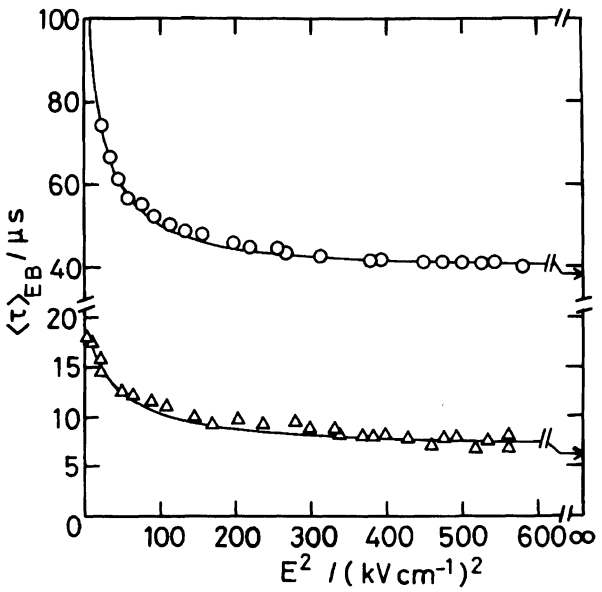

Fig. 6. Dependence of the rotational relaxation time on the electric field strength for $(A)_n\cdot(A^+)_n$ and $(A)_n\cdot(U)_n$. (○): $(A)_n\cdot(A^+)_n$ ($M_w=1.88\times10^5$, $M_w/M_n=1.52$, Mg^{2+}, $I_s=0.0004$). (△): $(A)_n\cdot(U)_n$ ($M_w=1.21\times10^5$, $M_w/M_n=1.46$, Mg^{2+}, $I_s=0.0004$). Solid line represents results calculated from Eq. 8 for each sample under consideration of the electric properties and molecular weight distributions of each sample given in Table 1.

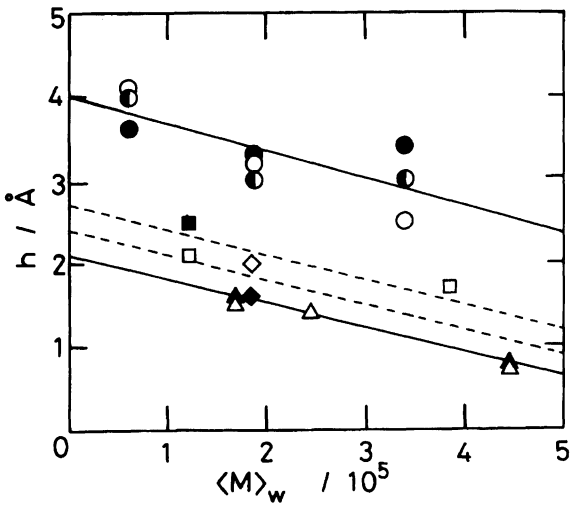

Fig. 7. Dependence of the axial translation per base-pair, h, on weight-averaged molecular weight, M_w, for four duplexes with counter ion Na^+ or Mg^{2+}. $(A)_n\cdot(A^+)_n$: (○) (Na^+, $I_s=0.0001$); (○) (Na^+, $I_s=0.001$); (●) (Mg^{2+}, $I_s=0.0001$). $(C)_n\cdot(C^+)_n$: (△) (Na^+, $I_s=0.001$ and 0.0008); (▲) (Mg^{2+}, $I_s=0.001$ and 0.0008). $(A)_n\cdot(U)_n$: (□) (Mg^{2+}, $I_s=0.001$); (■) (Mg^{2+}, $I_s=0.0004$). $(G)_n\cdot(C)_n$: (◇) (Na^+, $I_s=0.0008$); (◆) (Mg^{2+}, $I_s=0.0008$). Solid lines are obtained by the least-squared method for $(A)_n\cdot(A^+)_n$ and $(C)_n\cdot(C^+)_n$. Broken lines are drawn in parallel to the solid lines for $(A)_n\cdot(U)_n$ and $(G)_n\cdot(C)_n$.

versing-pulse birefringence signal shows no dip.

Figure 9a shows the dependence of the permanent dipole moment per unit length, $\langle\mu\rangle_w/\langle L\rangle_w$, of $(A)_n\cdot(A^+)_n$and $(C)_n\cdot(C^+)_n$ on $\langle L\rangle_w$. The $\langle\mu\rangle_w/\langle L\rangle_w$ are 0.43±0.18 debye Å^{-1}. The diverseness is small, regardless of the difference in the base-pairs, the chain length and the ionic strength. These results indicate that the magnitude of the permanent dipole moment of each backbone per unit length is ca. 0.2 debye Å^{-1}, and that the base-pairs do not contribute to the permanent dipole moment projected on the helix axis. Figure 9b shows the dependence of the saturable induced dipole moment per unit length, $\langle\Delta\sigma\rangle_w\langle E_0\rangle_w/\langle L\rangle_w$ on $\langle L\rangle_w$ for $(A)_n\cdot(A^+)_n$, $(C)_n\cdot(C^+)_n$, $(A)_n\cdot(U^+)_n$, and $(G)_n\cdot(C)_n$. These electric dipole moments are from 1.1 to 9.1 debye Å^{-1}, and the average values is 4.2 debye Å^{-1}. They are approximately independent of the chain length, probably because the saturable electrical anisotropy ($\langle\Delta\sigma\rangle_w$) increases, though the critical field strength ($\langle E_0\rangle_w$) decreases along with an increase in the chain length; thus, these two factors compensate for each other.

Figure 10a shows the dependence of the unsaturable induced electric anisotropy ($\langle\Delta\alpha\rangle_w$) on the chain length together with solid lines drawn by the least-squares method. At an ionic strength of 0.0001, the slopes are two for $(A)_n\cdot(A^+)_n$ with counter ions Na^+ (circles) and Mg^{2+} (squares). Thus, unsaturable induced electric dipole moment is proportional to the second power of the chain length. $\langle\Delta\alpha\rangle_w$ values for the Mg^{2+} counter ion are larger than those for Na^+. This trend may be related to the polymeric aggregation at an ionic strength

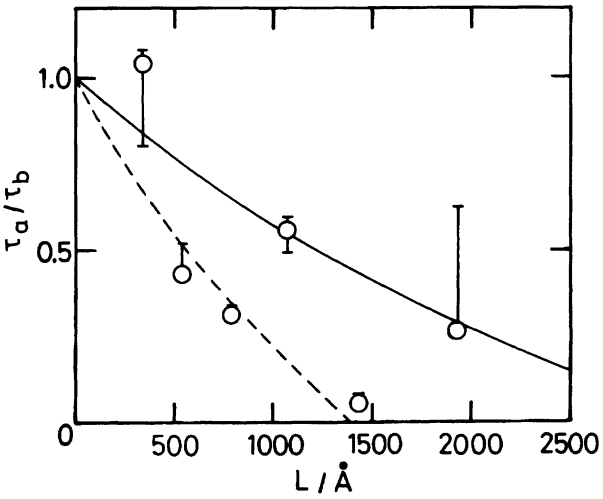

Fig. 8. Plot of τ_a/τ_b as a function of contour length L. τ_a is the experimental rotational relaxation time, τ_b is the rotational relaxation time for a straight cylinder of axial length, L. $(A)_n\cdot(A^+)_n$: (○); $(C)_n\cdot(C^+)_n$: (●). Solid line is obtained by calculation with Eq. 12, where a persistent length is 550 Å, while dashed line is obtained by calculation with Eq. 12, where a persistent length is 250 Å.

Table 2. Hydrodynamic Properties of Four Kind of Polyribonucleic Acids

Duplexes	Counter ions	Ionic strengths	τ / μs	L / Å	h / Å
Poly(A)·Poly(A^+)					
$M_w=3.39\times10^5$	Na^+	0.0001	80	1200	2.5
(1.53)[a]		0.0010	130	1400	3.0
	Mg^{2+}	0.0001	190	1600	3.4
		0.0010	1500	3400	7.1
$M_w=1.88\times10^5$	Na^+	0.0001	38	860	3.2
(1.52)		0.0004	38	860	3.2
		0.0010	30	790	3.0
	Mg^{2+}	0.0001	39	870	3.3
		0.0004	39	870	3.2
		0.0010	300	1800	6.8
$M_w=5.97\times10^4$	Na^+	0.0001	2.4	350	4.1
(1.34)		0.0010	2.3	340	4.0
	Mg^{2+}	0.0001	1.8	310	3.6
		0.0010	26	850	10
Poly(C)·Poly(C^+)					
$M_w=4.47\times10^5$	Na^+	0.0010	5.7	500	0.7
(1.56)	Mg^{2+}	0.0010	8.0	570	0.8
$M_w=2.45\times10^5$	Na^+	0.0008	5.3	510	1.4
(1.33)	Mg^{2+}	0.0008	5.7	520	1.4
$M_w=1.69\times10^5$	Na^+	0.0010	3.0	400	1.5
(1.39)	Mg^{2+}	0.0010	3.5	420	1.6
Poly(A)·Poly(U)					
$M_w=3.85\times10^5$	Mg^{2+}	0.0010	35	950	1.7
(1.35)					
$M_w=1.21\times10^5$	Mg^{2+}	0.0004	6.5	450	2.5
(1.46)		0.0010	4.0	370	2.1
Poly(G)·Poly(C)					
$M_w=1.85\times10^5$	Na^+	0.0008	8.0	530	2.0
(1.58)	Mg^{2+}	0.0008	4.4	430	1.6

a) Values in parentheses are the polydispersity M_w/M_n.

of 0.001 for Mg^{2+}. This aggregation mechanism must be open for future studying. At an ionic strength of 0.001 for the Na^+ counter ion, the slope is 0.6 (triangles); the effect of the chain length on the unsaturable induced dipole moment is less notable. Figure 10b shows the dependence of the critical electric field strength ($\langle E_0\rangle_w$) on the chain length ($\langle L\rangle_w$) for the $(A)_n\cdot(A^+)_n$ duplex. The solid line was drawn by the least-squares method. $\langle E_0\rangle_w$ is inversely proportional to the 1.5th power of $\langle L\rangle_w$, being independent of both the counter-ion species and the ionic strengths. The critical field strength is lower for $(A)_n\cdot(A^+)_n$ than for other duplexes. This may be due to the difference between the electric field surrounding the $(A)_n\cdot(A^+)_n$ duplex chain and that of other samples. The charge density of the backbone is smaller for $(A)_n\cdot(A^+)_n$ than for the other three duplexes because the axial translation of $(A)_n\cdot(A^+)_n$ is larger.

Calculation from Manning Theory. Manning[13,14] derived the following equation for the Debye–Hückel ion-atmosphere polarizability anisotropy for a macroion with univalent sites in a univalent-univalent salt solution:

$$\alpha_{//}-\alpha_{\perp}=\left(\frac{2q^2L}{hkT}\right)\left(\frac{3(1-a)}{2a+1}\right)\left(\frac{u_p}{u_s}\right)\left(\frac{1}{\xi\kappa^2}\right), \quad (13)$$

where a is the anisotropy of the mobility of the polymer; this value is 1/2 for a infinitely long cylinder in a solvent with a Debye length much greater than its radius.[62] u_p and u_s are the electrophoretic mobility of the polymer and the salt, respectively; u_p/u_s was assumed to be 0.83 in this calculation.[14] ξ is the structural parameter of $2q^2/\varepsilon kTh$, where q is the proton charge, ε is the bulk dielectric constant of the solvent, k is the Boltzmann constant and T is the Kelvin temperature. κ is the Debye screening parameter, and equals $8\pi10^{-3}N_{AV}(q^2/\varepsilon kT)I$, where N_{AV} is the Avogadro constant and I is the ionic strength. The electric polarizability induced by the counter ions condensed on a polymer chain is given as follows:[14]

$$\sigma=\frac{1}{6}\frac{q^2L^3}{hkT}\frac{Z^2\theta_0}{1-2Z^2\xi\theta_0\ln\left(\frac{\kappa h}{2}\right)}, \quad (14)$$

where $\theta_0=|Z|^{-1}(1-|Z|^{-1}\xi^{-1})$; Z is the valence of counter ion. The saturated induced dipole moments, which is the product of the calculated saturable polarizability from Eq. 14 and the critical field strength (σE_0)

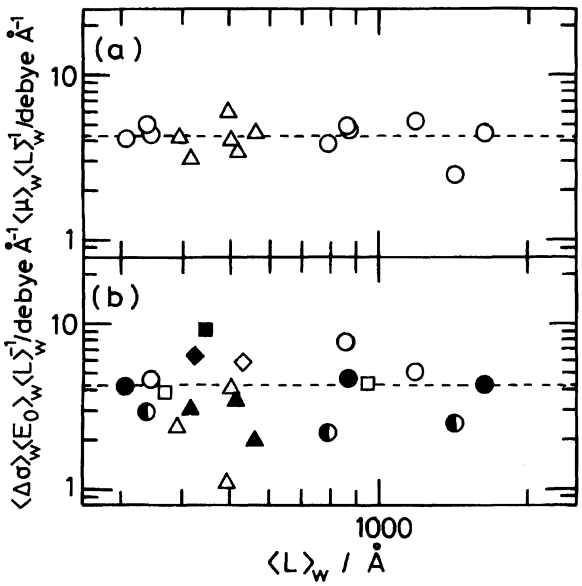

Fig. 9. Dependence of (a) the permanent and (b) saturated dipole moments on chain length of duplexes for four duplexes. $(A)_n\cdot(A^+)_n$: (○) (Na^+, I_s= 0.0001); (○) (Na^+, I_s=0.001); (●) (Mg^{2+}, I_s=0.0001). $(C)_n\cdot(C^+)_n$: (△) (Na^+, I_s=0.001, and 0.0008); (▲) (Mg^{2+}, I_s=0.001, and 0.0008). $(A)_n\cdot(U)_n$: (□) (Mg^{2+}, I_s=0.001); (■) (Mg^{2+}, I_s=0.0004). $(G)_n\cdot(C)_n$: (◇) (Na^+, I_s=0.0008); (◆) (Mg^{2+}, I_s= 0.0008).

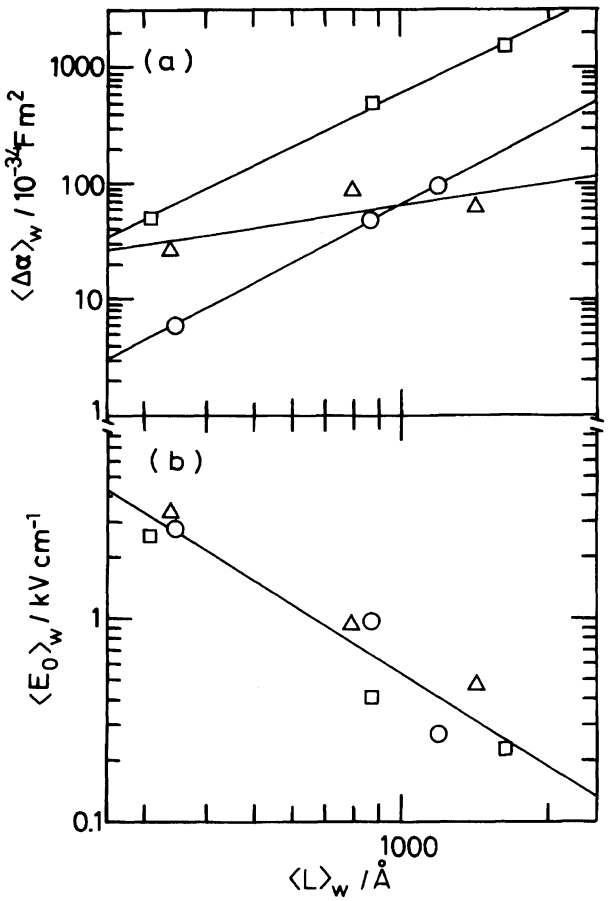

Fig. 10. Dependence of (a) the unsaturable induced electrical anisotropy and (b) the critical field strength on chain length of $(A)_n\cdot(A^+)_n$. (○) (Na^+, I_s= 0.0001); (△) (Na^+, I_s=0.001); (□) (Mg^{2+}, I_s= 0.0001). The solid lines are obtained by the least-squared method.

are given in Table 1.

Comparison with Manning Theory. Figure 11a shows the dependence of the calculated value from Eq. 14 (sclosed circles and closed triangles) and the experimental values (open circles and open triangles) of the unsaturable induced electric polarizability on the chain length for $(A)_n\cdot(A^+)_n$. A close agreement was obtained at an ionic strength of 0.001 (closed and open triangles). Thus, in this case the experimental result can be explained well by Manning's theory. When the ionic strength of Na^+ was ten-fold diluted to 0.0001, however, the calculated values (closed circles) were larger than the experimental ones (open circles); therefore, the unsaturable induced dipole moment was not only due to the Debye–Hückel ion-atmosphere polarizability, but also due to the polarizability of the counter ion condensed on the polymer.

Figure 11b shows the dependence of the saturated ion-induced dipole moment ($\Delta\sigma E_0$) on the chain length. A close agreement between the observed values (open symbol) and the calculated values with Eq. 14 (closed symbol) was obtained for the counter ion Na^+ at an ionic strength of 0.001. The experimental result for Na^+ at an ionic strength of 0.001 can be explained well by ion-condensed theory (Eq. 14). When the ionic strength is as low as 0.0001, the calculated value by Manning theory is smaller than the experimental value. The reason may be that a part of the polarizability of the counter ion condensed on a polymer does not saturate at E_0, and contributes to both the saturable and unsaturable induced electric polarizabilities. More detailed experimental work is necessary to show the details why the Manning theory cannot explain the experimental data in this region.

Conclusion

From the reversing-pulse birefringence signals of $(A)_n\cdot(A^+)_n$ and $(C)_n\cdot(C^+)_n$, which show a dip upon field reversal, these duplexes are thought to possess a permanent electric dipole moment. Both $(A)_n\cdot(U)_n$ and $(G)_n\cdot(C)_n$ duplexes possess no permanent dipole moment, because the reversing-pulse signals show no dip upon a field reversal. The axial translations per base-pair are 4.0 Å for $(A)_n\cdot(A^+)_n$, 2.7 Å for $(A)_n\cdot(U)_n$ and 2.4 Å for $(G)_n\cdot(C)_n$. From an analysis of the field-strength dependence of steady-state electric birefringence, the permanent dipole moments per unit length are found to be of the same value of 0.4 debye Å^{-1} for $(A)_n\cdot(A^+)_n$ and $(C)_n\cdot(C^+)_n$. These results indicate

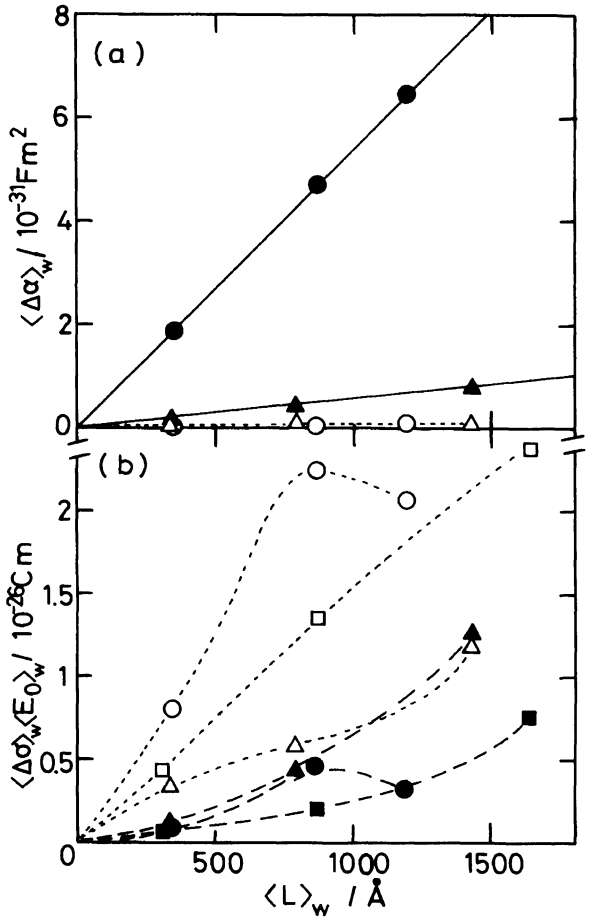

Fig. 11. Comparison of the electric properties of $(A)_n\cdot(A^+)_n$ between the experimental values (open symbols) obtained by using PD-SUSID orientation function and calculated values (closed symbols) by Manning's theory. (a) The unsaturable induced electrical anisotropy and (b) the saturated induced dipole moments, (○, ●) (Na^+, I_s=0.0001); (△, ▲) (Na^+, I_s=0.001).

that the magnitude of the permanent dipole moment of each backbone per unit length is 0.2 debye Å^{-1} and that the base-pair contributes slightly to the permanent dipole moment. It became clear from Manning theory that the unsaturable induced dipole moment ($\Delta\alpha E$) originates from the polarization of the Debye–Hückel ion-atmosphere and that the saturated induced dipole moment ($\Delta\sigma E_0$) is due to a condensation of the counter ions on the polymers. However, Manning theory is not applicable in such an extremely low ionic strength as 0.0001.

We gratefully acknowledge many helpful discussions with Mr. Kiyohiro Fukudome of this laboratory during the early stage of the present work. This work was in part supported by a Grant-in-Aid for Scientific Research (A) No. 02405008 from the Ministry of Education, Science and Culture.

References

1) M. Mandel, *Mol. Phys.*, **4**, 489 (1961).
2) F. Oosawa, *Biopolymers*, **9**, 677 (1970).
3) F. Oosawa, "Polyelectrolytes," Marcel Dekker, Inc., New York, N.Y. (1971), Chap. 5.
4) B. G. Archer, C. L. Craney, and H. Krakauer, *Biopolymers*, **11**, 781 (1972).
5) D. C. Rau and E. Charney, *Biophys. Chem.*, **14**, 1 (1981).
6) M. L. Bret and B. H. Zimm, *Biopolymers*, **23**, 271 (1984).
7) M. Fushiki, B. Svensson, BO Jönsson, and C. E. Woodward, *Biopolymers*, **31**, 1149 (1991).
8) M. Yoshida, K. Kikuchi, T. Maekawa, and H. Watanabe, *J. Phys. Chem.*, **96**, 2365 (1992).
9) G. Lamm, L. Wong, and G. R. Pack, *Biopolymers*, **34**, 227 (1994).
10) G. S. Manning, *Q. Rev. Biophys.*, **11**, 179 (1978).
11) G. S. Manning, *Biophys. Chem.*, **9**, 65 (1978).
12) G. S. Manning, *Biophys. Chem.*, **7**, 95 (1977).
13) G. S. Manning, *J. Chem. Phys.*, **90**, 5704 (1989).
14) G. S. Manning, *J. Chem. Phys.*, **99**, 477 (1993).
15) I. Tinoco, Jr., *J. Am. Chem. Soc.*, **77**, 4486 (1955).
16) I. Tinoco, Jr., and K. Yamaoka, *J. Phys. Chem.*, **63**, 423 (1959).
17) C. T. O'Konski, K. Yoshioka, and W. H. Orttung, *J. Phys. Chem.*, **63**, 1558 (1959).
18) S. Z. Jakabhazy and S. W. Fleming, *Biopolymers*, **4**, 793 (1966).
19) K. Yamaoka and E. Charney, *Macromolecules*, **6**, 66 (1973).
20) K. Yamaoka, K. Matsuda, and K. Takarada, *Bull. Chem. Soc. Jpn.*, **56**, 927 (1983).
21) K. Yamaoka and K. Matsuda, *J. Phys. Chem.*, **89**, 2779 (1985).
22) K. Yamaoka, S. Yamamoto, and I. Kosako, *Polym. J.*, **19**, 951 (1987).
23) K. Yamaoka and K. Fukudome, *J. Phys. Chem.*, **92**, 4994 (1988).
24) K. Yamaoka and K. Fukudome, *J. Phys. Chem.*, **94**, 6896 (1990).
25) K. Yamaoka, M. Kimura, and M. Okada, *Bull. Chem. Soc. Jpn.*, **65**, 129 (1992).
26) K. Kikuchi and K. Yoshioka, *Biopolymers*, **15**, 583 (1976).
27) K. Yoshioka, *Prog. Colloid Polym. Sci.*, **68**, 122 (1983).
28) D. C. Rau and E. Charney, *Macromolecules*, **16**, 1653 (1983).
29) K. Yoshioka, *J. Chem. Phys.*, **79**, 3482 (1983).
30) M. Tanigawa, K. Fukudome, and K. Yamaoka, *J. Sci. Hiroshima Univ. Ser. A*, **58**, 123 (1994).
31) A. Rich and D. R. Davies, *J. Am. Chem. Soc.*, **78**, 3548 (1956).
32) J. R. Fresco and P. Doty, *J. Am. Chem. Soc.*, **79**, 3928 (1957).
33) R. F. Steiner and R. F. Beers, Jr., *Biochem. Biophys. Acta*, **32**, 166 (1959).
34) A. Rich, D. R. Davies, F. H. C. Crick, and J. D.

Watson, *J. Mol. Biol.*, **3**, 71 (1961).
35) E. O. Akinrimisi, C. Sander, and P. O. P. Ts'o, *Biochemistry*, **2**, 340 (1963).
36) R. Langridge and A. Rich, *Nature*, **198**, 725 (1963).
37) G. D. Fasman, C. Lindblow, and L. Grossman, *Biochemistry*, **3**, 1015 (1964).
38) K. A. Hartman, Jr., and A. Rich, *J. Am. Chem. Soc.*, **87**, 2033 (1965).
39) W. Guschlbauer, *Proc. Natl. Acad. Sci. U.S.A.*, **57**, 1441 (1967).
40) A. J. Adler, L. Grossman, and G. D. Fasman, *Biochemistry*, **8**, 3846 (1969).
41) C. L. Stevens and G. Felsenfeld, *Biopolymers*, **2**, 293 (1964).
42) F. Pochon and A. M. Michelson, *Proc. Natl. Acad. Sci. U.S.A*, **53**, 1425 (1965).
43) R. D. Blake, J. Massoulié, and J. R. Fresco, *J. Mol. Biol.*, **30**, 291 (1967).
44) S. Arnott, D. W. L. Hukins, S. D. Dover, W. Fuller, and A. R. Hodgson, *J. Mol. Biol.*, **81**, 107 (1973).
45) R. O. Day, N. C. Seeman, J. M. Rosenberg, and A. Rich, *Proc. Natl. Acad. Sci. U.S.A.*, **70**, 849 (1973).
46) M. Tanigawa, N. Mukaiyama, S. Shimokubo, K. Wakabayashi, Y. Fujita, K. Fukudome, and K. Yamaoka, *Polym. J.*, **26**, 291 (1994).
47) K. Fukudome, K. Yamaoka, K. Nishikori, T. Takahashi, and O. Yamamoto, *Polym. J.*, **18**, 71 (1986).
48) K. Fukudome, K. Yamaoka, K. Nishikori, H. Tatehata, and O. Yamamoto, *Polym. J.*, **18**, 81 (1986).
49) A. Rich and M. Kasha, *J. Am. Chem. Soc.*, **82**, 6197 (1960).
50) G. C. Causley and W. C. Johnson, Jr., *Biopolymers*, **21**, 1763 (1982).
51) J. Brahms, A. M. Michelson, and K. E. Van Holde, *J. Mol. Biol.*, **15**, 467 (1966).
52) D. B. Lerner and D. R. Kearns, *Biopolymers*, **20**, 803 (1981).
53) K. Yamaoka and Y. Hino, *Bull. Chem. Soc. Jpn.*, **62**, 251 (1989).
54) K. Yoshioka and H. Watanabe, "Physical Prinsiples and Tecniques of Protein Chemistry," Part A, ed by S. J. Leach, Academic Press, New York, N.Y. (1969), Chap. 7.
55) S. Broersma, *J. Chem. Phys.*, **32**, 1626 (1960).
56) K. Matsuda and K. Yamaoka, *Bull. Chem. Soc. Jpn.*, **55**, 1727 (1982).
57) K. Yamaoka and K. Fukudome, *Bull. Chem. Soc. Jpn.*, **56**, 60 (1983).
58) K. Yamaoka and K. Matsuda, *Macromolecules*, **13**, 1558 (1980).
59) K. Ueda, *Bull. Chem. Soc. Jpn.*, **57**, 2703 (1984).
60) K. Yamaoka, K. Fukudome, and K. Matsuda, *J. Phys. Chem.*, **96**, 7131 (1992).
61) P. J. Hagerman and B. H. Zimm, *Biopolymers*, **20**, 1481 (1981).
62) M. Fixman and S. Jagannathan, *J. Chem. Phys.*, **75**, 4048 (1981).